[5] See, e.g. He G, Singisetti U, Ramamoorthy H, Somphonsane R, Bohra G, Matsunaga M, Higuchi A, Aoki N, Najmaei S, Gong Y, Zhang X, VAjtai R, Ajayan P M, and Bird J P 2015 *Nano Lett*. 15 5052,and references therein
[6] Ferry D K 1975 *Phys. Rev. B* 12 2361
[7] Ferry D K 2016 *Semicond. Sci. Technol*. 31 11LT01
[8] The notation here is that of Slater J C 1965 Quantum Theory of Molecules and Solids Vol. 2 (New York: McGraw-Hill) p 347 ff; others have used the notation Q for this point
[9] Curby R C and Ferry D K 1973 Phys. Stat. Sol. (a) 15 319
[10] Kaasbjerg K, Thygesen K S and Jacobsen K W 2012 *Phys. Rev. B* 85 115317
[11] Ferry D K 1991 Semiconductors (New York: Macmillan) Sec. 11.1

Stark effect in the photoluminescence of transition metal dichalcogenide structures

K-C Wang[1], T K Stanev[1], D Valencia[1], J Charles[1], P Sarangapani[1], A Henning[2], V K Sangwan[2], A Lahiri[1], M Povolotskyi[1], A Afzalian[3], G Klimeck[1], M Lundstrom[1], M C Hersam[2], L J Lauhon[2], N P Stern[1], and T Kubis[1]

[1]Purdue University, USA, [2]Northwestern University, USA, [4]TSMC, Belgium

Transition metal dichalcogenides (TMDs) are promising material candidates for next generation nanodevices due to few-atom device thickness and best imaginable gate control. In contrast to e.g. graphene, TMD offers a finite band gap which makes it suitable for transistors [1]. Van der Waal bonded layers are interesting for thin and flexible photovoltaics [2]. To identify the interlayer coupling, the band structure variation with different layer thicknesses and its gate field dependence is assessed here.

The electronic Hamiltonian and basis functions of density functional theory simulations (GGA with PBE [3] using the VASP software [4]) are used (within the Wannier90 software [5]) to extract an electronic Hamiltonian of a TMD unit cell in MLWF representation. This unit cell Hamiltonian is repeated in the NEMO5 software [6] to generate a real-size device Hamiltonian and solve for electronic densities. For charge self-consistency, the Schrödinger equation is iteratively solved with the Poisson equation in sub-atomic resolution, simplifying the spatial shape of Wannier functions with Gaussian functions (σ =0.6 Å). All assessed structures are close to the experimental setups of Ref. [2] with the same oxide capacitance and gate voltage.

The equivalent oxide thickness is set to be 300nm. The channel consists of one to ten layers of MoS_2 with doping deducted from current measurement. On the gate side, a Dirichlet boundary condition is used to set the gate voltage value. The top side is exposed to vacuum and a Neumann boundary condition of flat band (zero electric field) is applied.

Using the relaxed lattice, MLWF-calculated bandstructures are found to agree with ab-initio calculations for any TMD layer thickness [7]. The conduction band minimum in 2D momentum space is shown in in agreement with Ref.[9] Two inequivalent valleys exist with non-isotropic and layer dependent effective masses (in agreement with Ref.[9]), K and Q valley are the lowest for the conduction while K and Γ highest for the valence band. With increasing layer thickness, the bandedge shifts from K to Q (K and Γ) valley around 2 layer for the conduction(valence) bands as shown in Fig. 2. Fig. 3 compares the bandstructure of a 5-layer thick MoS2 system with and without a finite gate bias applied. Without electric fields, the K-valley is 5-fold degenerate. The finite gate field lifts this degeneracy and reduces the energy separation between K and Q valleys. This indicates the wavefunction localization differs for different valleys and the bandgap is tunable with electric gate fields. This is observed in Fig. 4 with a red shift of the PL spectrum – in good agreement with experimental data.

The nanodevice simulation tool NEMO5 was altered to accurately describe TMD in MLWF representation with ab-initio accuracy. Distinct valleys are tunable with layer thickness and applied gate voltage. Localized wavefunction of the K valley can cause a stark effect measurable with PL.

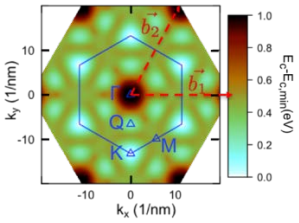

Fig. 1. Contour graph of the minimum of the conduction band for mono-layer MoS_2. The red hexagon depicts the first Brillouin zone.

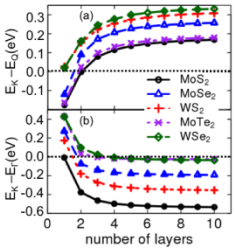

Fig. 2. Energy difference between the (a) K and Q valleys of the conduction band and (b) K and Γ for the valence band of different number of layer TMDs.

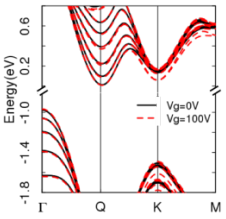

Fig. 3. Bandstructures of a 5-layer MoS_2 with and without finite gate voltage. The gate field lifts the degeneracy at the K valley while other valley unaltered.

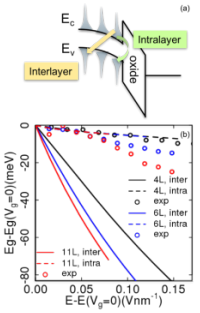

Fig. 2. (a) Schematic of the inter-layer and intra-layer bandgaps extraction. (b) The direct bandgap is biased via gate voltage. Both interlayer and intralayer bandgaps are extracted for 4,6, and 11 layers with different electric field at the oxide interface. Experiemntal bandgaps extracted from the PL measurement shows closer shifting to the intralayer bandgap.

[1] B. Radisavljevic, A. Radenovic, J. Brivio, V. Giacometti, and A. Kis, Nat. Nanotechnol. 6, 147 (2011).

[2] S. L. Howell, D. Jariwala, C.-C. Wu, K.-S. Chen, V. K. Sangwan, J. Kang, T. J. Marks, M. C. Hersam, and L. J. Lauhon, Nano Lett. 15, 2278 (2015).
[3] J. Perdew, K. Burke, and Y. Wang, Phys. Rev. B 54, 16533 (1996).
[4] G. Kresse and J. Furthmüller, Phys. Rev. B 54, 11169 (1996).
[5] N. Marzari and D. Vanderbilt, Phys. Rev. B 56, 12847 (1997).
[6] S. Steiger, M. Povolotskyi, H. H. Park, T. Kubis, and G. Klimeck, *IEEE Trans. Nanotechnol.* 10, 1464 (2011).
[7] Á. Szabó, R. Rhyner, and M. Luisier, Phys. Rev. B 92, 1 (2015).
[8] F. Jellinek, G. Brauer, and H. Müller, *Nature* 185, 376 (1960).
[9] H. Heo, J. H. Sung, S. Cha, B.-G. Jang, J.-Y. Kim, G. Jin, D. Lee, J.-H. Ahn, M.-J. Lee, J. H. Shim, H. Choi, and M.-H. Jo, *Nat. Commun.* 6, 7372 (2015).

Theoretical study of charge transport in mono- and bi-layer phosphorene using full-band Monte Carlo simulations

G Gaddemane, W G Vandenberghe, and M V Fischetti

The University of Texas at Dallas, USA

Phosphorene, single- or few-layer black phosphorous, has been recently added to the family of two-dimensional (2D) materi- als of interest for nanoelectronics applica- tions. Indeed, phospohorene, like graphene and unlike buckled 2D materials, maintains horizontal (σh) symmetry. Therefore, the cou- pling between electrons/holes and out-of- plane acoustic (ZA) phonons vanishes at first order [1], [2], thus suggesting good phonon- limited charge transport properties. However, reported theoretical estimates of the carrier mobility appear to be excessively optimistic. Indeed, the Bardeen-Shockley deformation potential theorem [3], used to evaluate the electron-phonon coupling, despite its suc- cess when applied to well-known materials, often ignores the anisotropy of the matrix elements and wavefunction overlap-integral. Using such a simplified form of the defor- mation potentials, and also considering only acoustic intravalley processes, mobilities in the range of 700-1100 (300-600) cm^2/Vs have been calculated for electrons (holes) in mono- layers [4], [5]. On the contrary, calculations performed by employing the full matrix elements yield significantly less satisfactory re- sults, $\approx$172 cm^2/Vs for both electrons and holes [6]. Here, by implementing full *ab initio*- based electron/hole-phonon scattering on an extremely fine grid and using the Monte Carlo method, we calculate the phonon-limited mo- bility and high-field characteristics for mono-layer and bilayer phosphorene.

Electron and phonon dispersion. In our study, we obtain the band-structure (Fig. 1) from the density-functional theory (DFT) Vi- enna *Ab initio* Simulation Package (VASP) [7] and phonon spectra (Fig. 2) from the PHONOPY computer program [8]. The relaxed lattice constants obtained are 4.62 A˚ and 3.30 A˚ for mono-layer and 4.52 A˚ and 3.30 A˚ for bi-layer phosphorene. The estimated band gaps are 0.90 eV and 0.50 eV for mono- and bi-layers, respectively. For the bi-layer, the Van der Waals gap obtained is 3.50 A˚ . We find low energy optical modes in bi-layer which are inter-layer modes. Two *k*- space grids, fine and coarse (0.004$A^{\circ -1}$ and 0.013 $A^{\circ -1}$) for the electronic band structure and 0.013 $A^{\circ -1}$ for the phonons) created on the Brillouin Zone, has been used to calculate and tabulate the electronic and phonon dispersions.

Calculation of electron-phonon scattering rates. The scattering rates are calculated numerically using Fermi's Golden rule. The deformation potentials are calculated by full *ab initio* calculations [9] on two grids, fine and coarse, with a size of 0.04 $A^{\circ -1}$ and 0.16 $A^{\circ -1}$ respectively. The density of states is computed using